HHS Public Access

Author manuscript

NPJ Aging Mech Dis. Author manuscript; available in PMC 2016 December 05.

Published in final edited form as:

NPJ Aging Mech Dis. 2016 ; 2: . doi:10.1038/npjamd.2016.19.

Extracellular Vesicle-Associated Aβ Mediates Trans-Neuronal Bioenergetic and Ca^{2+}-Handling Deficits in Alzheimer's Disease Models

Erez Eitan[1], **Emmette R. Hutchison**[1], **Krisztina Marosi**[1], **James Comotto**[1], **Maja Mustapic**[1], **Saket M. Nigam**[1], **Caitlin Suire**[1], **Chinmoyee Maharana**[1], **Gregory A. Jicha**[2], **Dong Liu**[1], **Vasiliki Machairaki**[3], **Kenneth W. Witwer**[4], **Dimitrios Kapogiannis**[1], and **Mark P. Mattson**[1,5,*]

[1]Laboratory of Neurosciences, National Institute on Aging, NIH, Baltimore, Maryland 21224.

[2]Sanders-Brown Center on Aging, and Department of Neurology, University of Kentucky College of Medicine, Lexington, KY 40508.

[3]Department of Pathology, Johns Hopkins University School of Medicine, 720 Rutland Avenue, Baltimore, MD 21205.

[4] Department of Molecular and Comparative Pathobiology and Department of Neurology, Johns Hopkins University School of Medicine, Baltimore, MD

[5]Department of Neuroscience, Johns Hopkins University School of Medicine, 725 N. Wolfe Street, Baltimore, MD 21205.

Abstract

Alzheimer's Disease (AD) is an age-related neurodegenerative disorder in which aggregation-prone neurotoxic amyloid β-peptide (Aβ) accumulates in the brain. Extracellular vesicles (EVs) are small 50-150 nanometer membrane vesicles that have recently been implicated in the prion-like spread of self-aggregating proteins. Here we report that EVs isolated from AD patient CSF and plasma, from the plasma of two AD mouse models, and from the medium of neural cells expressing familial AD presenilin 1 mutations, destabilize neuronal Ca^{2+} homeostasis, impair mitochondrial function, and sensitize neurons to excitotoxicity. EVs contain a relatively low amount of Aβ but have an increased Aβ42/ Aβ40 ratio; the majority of Aβ is located on the surface of the EVs. Impairment of lysosome function results in increased generation EVs with elevated Aβ42 levels. EVs may mediate transcellular spread of pathogenic Aβ species and that impair neuronal Ca^{2+} handling and mitochondrial function, and may thereby render neurons vulnerable to excitotoxicity.

Keywords

Alzheimer's disease; amyloid β-peptide; exosomes; extracellular vesicles; glutamate; mitochondria

*Correspondence: mark.mattson@nih.gov. Phone, 410 558-8463.

Introduction

Alzheimer's Disease (AD) is a progressive neurodegenerative disease that accounts for 60-70% of cases of dementia in the aging population. The disease has two pathological hallmarks: extracellular amyloid β (Aβ) peptide aggregates that form extracellular plaques, and intracellular hyperphosphorylated Tau protein aggregates that form neurofibrillary tangles. Pathogenic forms of Aβ and Tau can impair synaptic function and trigger a series of events leading to neuronal death [1]. While the causes of Aβ and Tau aggregation and cytotoxicity in the common sporadic late-onset cases of AD are unclear, 1-5% of AD patients exhibit early-onset disease resulting from mutations in the amyloid precursor protein (APP) or presenilin 1 (PS1; an enzyme that cleaves APP to generate Aβ) [1,2]. Studies of the consequences of expressing AD PS1 and APP mutations in cultured cells and transgenic mice have provided insight into the molecular and cellular alterations underlying the pathogenesis of AD [3]. In particular, aggregating Aβ and Tau can impair mitochondrial function and perturb neuronal Ca^{2+} handling, thereby rendering synapses and neurons vulnerable to degeneration [4-8].

Recently, it has been suggested that pathogenic forms of Aβ and Tau can propagate between cells in a prion-like manner, such that a misfolded protein can pass from a donor to a recipient cell and serve as a seed for further protein conversion and aggregation [9,10]. While it has been shown that injection of Aβ from either biological or synthetic sources into the mouse brain can accelerate endogenous Aβ aggregation throughout the brain, the mechanism responsible for this propagation of the pathology is unclear [11]. Extracellular vesicles (EVs), small membrane vesicles released from all cell types and found in bodily fluids, are one potential mechanism by which misfolded proteins and protein aggregates might spread through tissues [12,13]. EVs can contain several aggregation-prone proteins responsible for neurodegenerative disease including Aβ [14], APP C-terminal fragments [15], Tau [16], α-synuclein [17], SOD1 [18] and the prion protein (PrP) [19]. Moreover, two EV markers, Alix and Flotillin, have been found in amyloid plaques, suggesting a role of EVs in plaque generation [14,20]. EVs are secreted by either direct budding of the plasma membrane or fusion of multivesicular bodies (MVB) with the plasma membrane [21]. MVB have been reported as an important site of Aβ generation, leading to the suggestion that EVs may also be a site of APP processing into Aβ [14,22]. Interestingly, EVs released by healthy neurons can interact with extracellular Aβ and facilitate its fibrillation and clearance by microglia [23-26].

While EVs from AD patients and various AD models contain some amount of Aβ [14,15,27] the contribution of EVs to Aβ production and the pathogenesis of AD is not clear. Here we report that EVs isolated from the cerebrospinal fluid (CSF) of patients with sporadic, late onset AD or released from cultured human neurons harboring a pathogenic PS1 mutation are toxic to cerebral cortical neurons by a mechanism involving EV surface-associated Aβ. EVs with neurotoxic Aβ impair neuronal Ca^{2+} handling and mitochondrial function. The release of EVs with neurotoxic Aβ is increased when lysosome function is compromised, suggesting that the impaired lysosome function that occurs in neurons in AD [28] may trigger EV-mediated transneuronal propagation of neurodegenerative cascades.

Results

Extracellular vesicles from PS1 mutant cells contain a relatively low concentration of Aβ, but are enriched in Aβ42 relative to Aβ40

To investigate the effects of pathogenic PS1 mutations on EV-associated Aβ, we first isolated EVs from the culture medium of H4 glioblastoma cell lines genetically engineered to express either the PS1Δ9 mutation ($H4^{PS1\Delta9}$) or wild type PS1 ($H4^{PS1WT}$) in an inducible manner. The expression of PS1Δ9 or PS1WT was induced by tetracycline for 5 days, and EVs were isolated from the culture medium by ultracentrifugation [29]. The EVs were evaluated according to the published guidelines [30] by transmission electron microscopy, immunoblot analysis and NTA particle size analysis (Figure 1A-D). The vast majority EVs were 50 – 250 nm in diameter, with the most abundant size being about 130 nm (Figure 1C). The EVs contained high amounts of the EV marker proteins flotillin-1 and CD9 (Figure 1D). We found that the PS1Δ9 mutation did not alter EV morphology, size distribution or expression of these EV markers. The levels of Aβ40 and Aβ42 associated with EVs and free in the culture medium were measured by a Mesoscale Discovery (MSD)® immunoassay (Figure 1E). Aβ40 and Aβ42 were significantly lower in the EV fraction than in the EV-depleted medium fraction and in the parent cell lysates (Figure 1E). Given that the Aβ42/Aβ40 ratio may be a better predictor of AD than the individual concentrations of Aβ40 and Aβ42, we calculated the Aβ42/Aβ40 ratio [31,32] and found that the Aβ42/Aβ40 ratio in EVs was significantly higher than in EV-depleted medium or cell lysate (Figure 1F).

To further characterize the association of Aβ with EVs, we examined EVs released from cultured human neurons derived from iPSC generated from fibroblasts taken from a patient with AD caused by a PS1 mutation ($hN^{PS1A246E}$ neurons) and control neurons generated from fibroblasts from a neurologically normal human subject [33]. EVs isolated from culture medium were evaluated by NTA and immunoblotting with antibodies against the EV markers flotillin-1 and CD9 (Supplemental Figure 1). The levels of Aβ42 and Aβ40 associated with EVs were significantly lower than Aβ42 and Aβ40 levels in the EV-depleted medium (Figure 1E), but the Aβ42/Aβ40 ratio was significantly higher in EVs compared to EV-depleted medium (Figure 1F). As expected, the levels of Aβ42 were higher in $H4^{PS1\Delta9}$ cell lysate, culture medium and EVs compared to $H4^{PS1WT}$ cells, and the level of Aβ42 was higher in $hN^{PS1A246E}$ medium than hN^{PS1WT} medium (Supplemental Figure 2).

We next determined whether EV-associated Aβ is contained within EVs and/or on the outer surface of their membrane. EVs were incubated with 1 mg/ml trypsin for 1 hour prior to two rounds of 120,000 × g centrifugation to purify EVs. The trypsin treatment reduced the amount of Aβ42 and Aβ40 associated with EVs isolated from $H4^{PS1\Delta9}$ cells by 82% (Figure 1G). These results indicate that most EV-associated Aβ is located on the outer surface of the EV membrane. It has been reported previously that neuronal EVs contain several Aβ-binding proteins and lipids [34-36]. Thus, it is possible that the Aβ is not released together with the EVs but becomes associated with EVs extracellularly. However, incubating EVs derived from $H4^{PS1WT}$ cells with EV-depleted medium derived from $H4^{PS1\Delta9}$ resulted in only a very small increase in the levels of EV-associated Aβ (Figure 1G), suggesting that Aβ becomes associated with vesicles prior to their release from cells.

Accumulating evidence indicates that Aβ production can occur in the endosomal system, including within MVBs [14,22,37]. We hypothesized that, if the association of Aβ with vesicles occurs in the endosomal system, inhibiting the lysosome would increase the release of Aβ42-containing EVs [38]. Incubating H4$^{PS1\Delta9}$ cells for 24 hours with 200 μM of bafilomycin A significantly increased EV secretion by 1.4 fold (data not shown), and the concentration of Aβ associated with EVs was increased by about 3 fold (Figure 1H); the Aβ42/Aβ40 ratio was also increased significantly (Supplemental Figure 3). Bafilomycin A is a V-ATPase inhibitor and, while being a potent inhibitor of lysosomal function, it also has an effect on endosomal pH levels which could effect the activity of β-secretase and γ-secretase [38,39]. Therefore, we measured the effect of bafilomycin A on Aβ concentration in the cells and culture medium. The level of Aβ in the cells was increased similarly to that in EVs, but there was no significant difference in the level of Aβ in culture media from control and bafilomycin A-treated cells (Supplemental Figure 3A). To verify the effect of lysosome inhibition on EV-associated Aβ, we employed Cas9 with a sgRNA targeted to disrupt the cathepsin D gene (Supplemental Figure 3B). H4 cells, in which cathepsin D was knocked down, secreted EVs with 3-fold more Aβ and had a higher Aβ42/Aβ40 ratio compared to EVs secreted from control H4 cells (Figure 1H and Supplemental Figure 3C).

EVs derived from PS1 mutant cells are neurotoxic

Having established that PS1 mutant neurons release EVs that have higher levels of Aβ on their surface, we performed a series of experiments to determine whether these EVs are neurotoxic. When EVs isolated from the culture medium of H4$^{PS1\Delta9}$ cells were added to primary rat cortical neurons at a concentration of approximately 300 EVs/neuron, significant reductions of neuronal viability occurred within 48 hours (Figure 2A, B). Interestingly, incubation of primary cortical neurons with EV-depleted medium (containing about 10-fold more Aβ42 than EVs) or with 10 μM of recombinant Aβ42 had a similar effect on neuronal viability as did the lower amount of Aβ associated with EVs released from cells expressing mutant PS1 (Figure 2A and B). It was previously reported that Aβ42 sensitizes neurons to glutamate-induced excitotoxicity [40]. We, therefore, determined if EVs isolated from the medium of mutant PS1-expressing cells affect the vulnerability of neurons to excitotoxicity. Cortical neurons were exposed to EVs for 24 hours, followed by the addition of 100 μM glutamate for an additional 24 hours. Parallel neuronal cultures were exposed to EVs, glutamate or vehicle for 48 hours. Glutamate alone induced a 15-20% reduction in viability, but in combination with EVs from H4$^{PS1\Delta9}$ cells, neuronal viability was reduced by 50-56% (Figure 2A and B). To further examine whether the neurotoxicity of H4$^{PS1\Delta9}$ derived EVs is mediated by Aβ, the ability of an antibody against Aβ (6E10) to protect neurons was examined; the Aβ antibody abolished the neurotoxicity of the EVs (Figure 2A and B). The latter result suggests that the neurotoxic property of EVs is mediated by Aβ on their surface.

To further investigate the neurotoxicity of EV-associated Aβ, we incubated neurons for 48 hours with EVs derived from H4$^{PS1\Delta9}$ cells followed by fixation and staining with Thioflavin S (to label Aβ aggregates with a β-sheet structure), and antibodies against cleaved-caspase 3 (a marker of apoptosis) and the neuron-specific cytoskeletal protein MAP2 (Figure 2C-F). The fluorescent intensities of both Thioflavin S and cleaved-caspase 3 were significantly greater (4- and 3.5- fold higher, respectively) in neurons treated with EVs

from $H4^{PS1\Delta9}$ cells compared to neurons treated with EVs from $H4^{PS1wt}$ cells, while the amount of MAP2 immunoreactivity was 40% lower (Figure 2F). The levels of Thioflavin S were also greater in neurons treated with $H4^{PS1wt}$ derived EVs compared to untreated neurons. To determine the relative numbers of EVs internalized by the neurons, EVs were stained with the lipophilic dye PKH26 before incubation with cortical neurons, and internalized EVs were imaged by confocal microscopy (Figure 2G). There was no apparent difference in the amount of $H4^{PS1\Delta9}$ and $H4^{PS1WT}$ EVs internalized by the neurons (Figure 2G and quantification in Supplemental Figure 4A). To better quantify the levels of internalization, different amounts of labeled EVs were added to the culture medium, and the increase in flourecence intensity was measured after 4 and 24 hours of incubation. EV concentration-dependent increases in internalization was seen at both time points (Supplemental Figure 4B and C). Incubating the labeled EVs with Aβ antibody only slightly reduced their internalization (Supplemental Fgure 4 B and C) and thus the ability of the antibody to completely block neurotoxicity is probably not due to reduced internalization. EVs from $hN^{PS1A246E}$ neurons were relatively less neurotoxic than EVs from $H4^{PS1\Delta9}$ cells (Figure 2H and I). This difference could be due to the two different PS1 mutations (PS1 A246E compared to PS1Δ9), to different amounts or conformations of Aβ42 on the EV surfaces, or to differential biological activities of the EVs independent of Aβ (for example, it has been reported that EVs released from stem cells have trophic effects [41]).

AD cell-derived exosomes cause calcium dysregulation and mitochondrial impairment, and can trigger neuronal apoptosis

To determine the cause of the observed neurotoxicity of EVs released from cells expressing AD mutant PS1, we examined the effects of these EVs on neuronal Ca^{2+} handling following glutamate exposure and on cellular metabolism using the Seahorse® mitochondrial function assay. Primary cortical neurons were incubated for 48 hours with EVs released from $H4^{PS1\Delta9}$ or $H4^{PS1wt}$ cells, or with EVs released from $hN^{PS1A246E}$ neurons. The $[Ca^{2+}]_I$ responses to glutamate in neurons treated with EVs from $H4^{PS1\Delta9}$, $H4^{PS1wt}$, hN^{PS1wt} neurons, $hN^{PS1A246E}$ neurons, or synthetic Aβ42 are shown in Figure 3A-F. Incubating neurons with EVs from PS1 mutant cells did not induce any increase in the magnitude of the peak $[Ca^{2+}]_I$ response (Figure 3B, E), but did cause a significant increase in the response duration (37% and 21% increases for EVs from $H4^{PS1\Delta9}$ cells and iPS neurons, respectively; Figure 3C and F). While adding the Aβ blocking antibody did not have an effect on amplitude of $[Ca^{2+}]_I$ response (Figure 3B), it did enhance recovery of $[Ca^{2+}]_I$ following glutamate exposure (Figure 3A and C), suggesting that the effect of EVs on recovery of $[Ca^{2+}]_I$ is mediated by the Aβ on the surface of the EVs. This analysis may underestimate the increase in $[Ca^{2+}]_I$ response duration caused by EVs, because the $[Ca^{2+}]_I$ in rat cortical neurons treated with EVs released from $H4^{PS1\Delta9}$ and iPSC-derived neurons did not recover to 50% of maximum (Figure 3G).

We next performed a Seahorse® mitochondrial function assay on neurons treated with EVs released from $H4^{PS1\Delta9}$ and $H4^{PS1wt}$ cells, and found significantly reduced mitochondrial functionality as a result of incubation with EVs released from cells expressing the PS1Δ9 mutation (Figure 3H and I). The effects of $H4^{PS1\Delta9}$ cell-derived EVs in reducing basal and maximal respiration, and ATP levels, were similar to the reductions in these mitochondrial

variables in neurons exposed to synthetic Aβ42 (Figure 3H and I). Collectively, the data are consistent with a role of EV surface-associated Aβ42 in the neurotoxic effects of EVs.

Extracellular vesicles in mouse models of AD and AD patient CSF exhibit a high Aβ42/40 ratio

To determine whether EVs isolated from biological fluids of AD patients and animal models exhibited Aβ-related neurotoxic properties similar to EVs release from cultured cells expressing mutant PS1, we measured the concentrations of Aβ42 and Aβ40 in EVs isolated from plasma samples from 6 transgenic APP/PS1 double mutant transgenic mice [42], 5 3xTgAD mice [43] and 9 age-matched wild type mice. The levels of Aβ42 and Aβ40 were significantly lower in EVs and EV-depleted plasma samples from wild type mice compared to transgenic mice (Supplemental Figure 5). The levels of Aβ42 and Aβ40 were significantly lower in plasma derived EVs than in EV-depleted plasma (Figure 4A), but the Aβ42/Aβ40 ratio was significantly higher in the EVs compared to EV-depleted plasma (Figure 4B). Next, we isolated EVs from CSF samples from 6 patients with sporadic, late-onset AD, 6 MCI patients, and 6 age-matched control subjects. EVs isolated from CSF were highly enriched in the EV markers flotillin-1 (FLOT1) and Alix (Supplemental Figure 6A), but not the intracellular (non-exosomal) protein early endosome antigen 1 (EEA1; data not shown). Interestingly, the EV size distribution in all CSF samples showed two populations, one with a mean diameter of about 70 nm, a size typical of exosomes, and another with a mean size of about 170 nm, which may be microvesicles [21]. The concentration of EVs in the CSF of AD, MCI and healthy individuals were similar and much lower than their concentration in plasma (Supplemental Figure 6D).

We next measured the levels of Aβ42 and Aβ40 in CSF-derived EVs and found that these were significantly lower in EVs compared to EV-depleted CSF and plasma samples of AD patients (Figure 4C). The Aβ42/Aβ40 ratio was significantly higher in EVs derived from CSF and plasma of AD patients compared to EV-depleted CSF and plasma samples (Figure 4D). The levels of Aβ42 and Aβ40 associated with EVs were also low in CSF samples from subjects with MCI and aged-matched neurologically normal healthy subjects, but the Aβ42/Aβ40 ratio was significantly higher in EVs isolated from AD patients CSF compared to EVs from control subjects CSF (Supplemental Figure 7). To determine if EV-associated Aβ from AD patient CSF was contained within EVs and/or on their surface, EVs were incubated with 1 mg/ml trypsin for 1 hour prior to two rounds of 120,000 × g centrifugation to purify EVs. Similar to EVs released from $H4^{PS1\Delta 9}$ cells (Figure 1G), we observed a 75% reduction in the amount of Aβ42 and Aβ40 associated with EVs treated with trypsin compared to EVs not treated with trypsin (Figure 4E).

CSF-derived exosomes cause calcium dysregulation and mitochondrial impairment and can trigger neuronal apoptosis

The finding of high Aβ42/Aβ40 ratio of CSF-derived EVs from patients with sporadic, late-onset AD prompted us to evaluate their potential neurotoxicity. EVs isolated from CSF were added to the medium bathing cultured cerebral cortical neurons (approximately 100 EVs/neuron), and 48 hours later cell viability was measured with MTT and LDH assays. Exposure of neurons to CSF-derived EVs resulted in a significant reduction of neuronal

viability in MTT (Figure 5A) and LDH (Figure 5B) assays. The magnitude of reduction of viability of CSF EV-treated neurons was similar to that measured in neurons exposed to 10 μM Aβ42, whereas EVs isolated from cultured rat cortical neurons exhibited no neurotoxicity (Figures 5D and E). Moreover, EVs isolated from the CSF of healthy human subjects did not induce significant toxicity (Supplemental Figure 7). CSF EVs from AD patients and synthetic Aβ42 significantly increased the vulnerability of cortical neurons to glutamate excitotoxicity, and these adverse effects of AD CSF EVs and synthetic Aβ42 were abolished by treatment with an Aβ antibody (Figure 5A, B). To determine if EVs from AD CSF cause Aβ aggregation and apoptosis, neurons were stained with thioflavin S and a cleaved-caspase 3 antibody (Figures 5C and D). Thioflavin S staining was undetectable in untreated neurons (not shown) and in neurons treated for 48 hours with EVs isolated from the medium of cultured rat cortical neurons, but was evident in neurons incubated for 48 hours with human CSF-derived EVs, and to a lesser extent in neurons treated with Aβ1-42 (Figure 5C). Whereas no neurons exhibited cleaved-caspase 3 immunoreactivity in cortical neuron cultures treated with EVs released from healthy cortical neurons, many neurons exhibited cleaved caspase 3 immunoreactivity in cortical neurons treated with AD CSF-derived EVs or Aβ42 (Figure 5C and D).

To provide further insight into the role of EV-associated Aβ in neuronal degeneration in AD, we plotted the concentration of Aβ42 in EVs isolated from cell culture medium and human subject CSF as a function of the relative neurotoxicity of EVs from the same sources (Supplemental Figure 8). The most neurotoxic EVs, those from AD patient CSF and those released from cells expressing mutant PS1, also had the highest amounts of Aβ42 associated with them. In contrast, EVs released from control human cells were the least neurotoxic and had the lowest amounts of Aβ42 associated with them. There was a highly significant correlation of EV Aβ42 level and neurotoxicity of the EVs (Supplemental Figure 8).

We next performed Ca^{2+} imaging experiments in which $[Ca^{2+}]_I$ responses to glutamate were measured in vehicle-treated control rat cortical neurons and in neurons that had been pre-incubated for 48 hours with CSF EVs from AD, MCI and control subjects, or Aβ42. Neurons incubated with AD CSF-derived EVs demonstrated a significant 25 ± 9% increase in the peak amplitude of the glutamate-induced elevation of $[Ca^{2+}]_I$; this effect of AD CSF EVs was prevented by treatment with an Aβ antibody (Figure 6A, B). The time required for the $[Ca^{2+}]_I$ to return to 50% of the peak $[Ca^{2+}]_I$ response to glutamate was not significantly affected by AD CSF EVs, although there was a trend towards slower recovery of $[Ca^{2+}]_I$ ($p<0.072$; Figure 6C). We next measured neuronal oxygen consumption to evaluate mitochondrial function in cortical neurons exposed for 48 hours to CSF EVs from AD, MCI and control subjects (Figure 6D shows the results of a representative experiment, and Figure 6E is combined data from 6 experiments). Neurons treated with AD patient CSF-derived EVs or with Aβ42 had significantly reduced basal and maximal respiration, and reduced ATP production (Figure 6E). The adverse effects of AD CSF EVs on mitochondrial function were abolished by treatment with an Aβ antibody (Figure 6E).

Discussion

We found that, compared to various control EVs, EVs released from cultured human neurons and cell lines expressing mutant PS1, and EVs isolated from the CSF of sporadic, late-onset AD patients, have elevated amounts of Aβ42 (predominantly located on their surface) and can induce degeneration of cerebral cortical neurons. EVs from sporadic, late-onset AD patient CSF and EVs released from cells expressing mutant PS1 impaired mitochondrial function, destabilized neuronal Ca^{2+} homeostasis, and rendered cortical neurons vulnerable to excitotoxicity. The adverse effects of the AD patient and experimental model EVs on neuronal Ca^{2+} handling, mitochondrial function and cell viability were prevented by treatment with an Aβ antibody, indicating a key role for EV surface-associated Aβ in pathogenic effects of AD EVs.

Our findings provide novel insight into potential roles of EVs in propagating Aβ–related pathology and associated neuronal degeneration. It has been suggested that AD pathology spreads in a trans-neuronal manner with prion-like characteristics [9,10], and this possibility is supported by data from mouse model experiments where inoculation with synthetic Aβ or Aβ-containing brain homogenate accelerate development of pathology [11]. Interestingly, we found that although the majority of Aβ in CSF, plasma and culture medium is not associated with EVs, the EVs have significantly higher Aβ42/Aβ40 ratio and are toxic to primary neurons, suggesting a possible role for EVs in AD pathogenesis. The toxic effect of EVs is specific to AD (even in sporadic, late-onset cases) or at least to neurodegenerative disease, because CSF EVs from healthy subjects exhibited little or no neurotoxicity.

We found that EVs isolated from CSF, plasma, and culture medium from human neural cells expressing pathogenic PS1 mutations contained lower concentrations of Aβ40 and Aβ42 compared to the fluid from which they were isolated. However, the Aβ42/Aβ40 ratio was significantly higher in EVs compared to the fluids from which they were isolated. These findings are of interest with regards to AD pathogenesis as the Aβ42/Aβ40 ratio has been found to be a more reliable biomarker for AD than Aβ42 or Aβ40 alone [44]. Moreover, mixtures of Aβ42 and Aβ40 with a higher Aβ42/Aβ40 ratio aggregate more vigorously and are more neurotoxic than mixtures with a low Aβ42/Aβ40 ratio [45,46]. It was recently reported that EVs of neuronal origin isolated from the blood of AD patients prior to their diagnosis contain elevated levels of Aβ42 (and p-Tau) compared to EVs from healthy control subjects [47]. We found that EVs have a relatively high Aβ42/40 ratio and are potent in disrupting neuronal Ca^{2+} homeostasis, impairing mitochondrial function and triggering apoptosis. However, whether Aβ associated with EVs plays a critical role in the pathogenesis of AD remains to be determined.

Recent findings suggest that EVs can transport pathogenic forms of Aβ, pTau and α-synuclein into recipient neurons via internalization [14,16,17]. We found that EVs isolated from sporadic, late-onset AD patient CSF, or from the culture medium of human cells expressing mutant PS1, are internalized by cerebral cortical neurons. The recipient neurons accumulate Thioflavin S-reactive protein aggregates, and manifest impaired Ca^{2+} handling and mitochondrial dysfunction. However, in contrast to the presumption that Aβ is located inside EVs [13], we found that Aβ1-42 is predominantly located on the external surface of EVs.

Previous findings suggest that Aβ aggregation is enhanced when the pathogenic peptide is associated with cell membranes, particularly membranes rich in sphingomyelin, gangl iosides and cholesterol, so-called lipid rafts [48-52]. During the process of its aggregation on the membrane surface, Aβ can generate reactive oxygen species that induce membrane lipid peroxidation [53,54], which can impair the function of membrane ion-motive ATPases, and glucose and glutamate transporters, and thereby render neurons vulnerable to excitotoxicity and apoptosis [55-57]. Our data suggest that similar to aggregating synthetic Aβ1-42, EV surface-associated Aβ can increase the vulnerability of neurons to excitotoxicity and apoptosis by a mechanism involving impaired Ca^{2+} regulation.

It has been suggested that neuronal EVs can scavenge extracellular Aβ by binding of Aβ to EV proteins such as cystatin c [35], insulin-degrading enzyme [34,58], the cellular prion protein [26] and ganglioside GM1 [36]. We incubated EVs derived from cells expressing wild type PS1 with EV-depleted medium from PS1Δ9 mutant cells and found a small but significant increase in Aβ associated with the EVs; however, Aβ levels in the latter EVs were considerably lower than EVs released from PS1Δ9 mutant cells. Our findings therefore suggest that while EVs have some capacity to interact with extracellular Aβ, much of the Aβ associated with EVs released from neural cells is present prior to their release. Accumulating evidence suggests that endosomes are a major site of APP processing to generate Aβ species [59]. Endosomes may therefore be relatively enriched in Aβ that may associate with the intraluminal vesicles that can then be released from cells as EVs (exosomes). It has been shown that aggregation of proteins on the plasma membrane can trigger membrane budding and release of EV containing high amounts of the aggregated protein [60]. Tetraspanins [61,62] and syndecan heparan sulfate proteoglycans, together with Alix and syntenin [63], are involved in the formation and release of such EVs. Hence, it is possible that Aβ aggregation on the plasma and/or endosomal membranes results in Aβ secretion with EVs, and that such EVs are enriched in Aβ42 and Aβ40 in amounts and a stoichiometry [45,46] that render them highly pathogenic.

In AD patients, active lysosomal proteases are associated with plaques and degenerating neurons, which also display other characteristics of lysosomal dysfunction including increased expression of hydrolases such as cathepsin D and accumulation of lysosomes [64,65]. Familial AD PS1 mutations disrupt lysosomal acidification and autophagy [66]. Cells in brain tissue samples from sporadic, late-onset AD patients also display a marked increase in immature autophagic vacuoles [67], a phenotype possibly related to lysosome impairment [28]. Disruption of autophagy through heterozygous deletion of Beclin1 in an AD mouse model resulted in both intracellular accumulation of Aβ and increased amyloid plaque deposition [68], suggesting that autophagy is a major facilitator of Aβ clearance. However, crossing an AD mouse model with a mouse line defective in autophagy (ATG7 knockout mice) resulted in accumulation of intracellular Aβ and reduced Aβ secretion [69], suggesting that autophagy may also play a role in Aβ secretion. Previous studies have shown that mutations in PS1 cause lysosome impairment [66], EVs contain lysosomal proteins [70], and EV marker proteins such as Alix and flotillin-1 are present in AD amyloid plaques [14,20]. We found that inhibition of autophagy (by exposure to bafilomycin A or CRISPR-Cas 9-mediated knockdown of cathepsin D) in cells expressing mutant PS1 resulted in increased release of EVs with elevated amounts of Aβ42, suggesting that impaired autophagy may

result in the release of pathogenic EVs in AD. These Aβ42–laden EVs are neurotoxic as indicated by their adverse effects on neuronal Ca^{2+} homeostasis, mitochondrial function, and vulnerability to excitotoxicity and apoptosis. Data from previous studies of postmortem brain tissue from sporadic, late-onset AD patients, and of experimental cell culture and animal models, strongly support roles for impaired neuronal Ca^{2+} handling, mitochondrial dysfunction and apoptosis-like cell death in AD [1,4,71]. Future studies involving animal models and human subjects will be required to elucidate the roles of Aβ-laden EVs in AD pathogenesis and their potential as a therapeutic target.

Materials and Methods

Animals

APP/PS1 double mutant transgenic mice (2xTg AD mice; B6C3-Tg(APPswe, PS1Δ9)85Dbo) [42] and 3xTgAD mice (B6 129-Psentm1Mpm Tg, APPSwe, tauP301L1Lfa) mice [43] were maintained under a 12 h light/12 h dark cycle with food and water available ad libitum. Mice were euthanized with an overdose of isoflurane anesthesia and blood was collected directly from the heart. All procedures were approved by the National Institute on Aging Animal Care and Use Committee and complied with NIH guidelines.

Cell Culture, experiments treatments, transfection and cell viability assays

Dissociated embryonic rat cortical cells cultures were established and maintained using methods similar to those described previously [72]. Neurons were grown in polyethylenmine-coated plastic culture dishes or cover slips. Cultures were maintained at 37°C (5% CO_2/95% air atmosphere) in Neurobasal medium (Gibco 21103-049) containing B-27 supplement (Invitrogen) plus 1% antibiotic (Gibco 15240-062). One quarter of the medium was replaced every 3 days and the cells were maintained for 7-10 days in culture prior to performing experiments. Human neuroglioma (H4TR) cells stably expressing wild type (WT) PS1 or mutant PS1 (delta E9 mutation) under the control of a tetracycline responsive element were cultured in Dulbecco's modified Eagle medium (DMEM, Gibco # 12800-058) supplemented with 10% fetal bovine serum (Tet-tested, Thermoscientific # SH30070.03T), 50 μg/ml Zeocin (Invitrogen, #R250-01) and 2.5 μg/ml blasticidin (Invitrogen, #R210-01), and were maintained at 37°C (5% CO_2/95% air atmosphere). To induce expression of the mutant form of PS1, the cells were induced with 100 ng/ml tetracycline (Sigma #T7660) for 3-5 days. Human neurons were differentiated from induced pluripotent stem cells (iPSC) that had been derived from fibroblasts taken from a patient with early-onset AD caused by a PS1 mutation (A246E) using methods described previously [33].

Cells were grown to 50-60% confluency prior to transfection. The following plasmids were transfected using Lipofectamine LTX (Invitrogen 94756) according to the manufacturer's protocol: Rab11-FIP3 CRISPR/Cas9 Double Nickase (sc-405735-NIC) and cathepsin D CRISPR/Cas9 (sc-400207). Bafilomycin A (Baf A) was dissolved in dimethylsulfoxide to generate a stock solution of 400 mM and stored at −20°C. When thawed, the Baf A was diluted 1:2000 in cell culture medium. In order to examine effects on cell viability, rat primary neurons were plated in a 96 well plate (30,000 cells per well) and treated as indicated. Neurons were exposed to EVs isolated from CSF or plasma (at a concentration

calculated to result in a EV/neuron ratio of 100:1) or H4-derived EVs (EV/neuron ration of 300:1) for 48 hours, and in some experiments 100 μM glutamate was added after 24 hours of EV treatment. Following 48 hours EV incubation, 50 μl of medium was taken from each well and centrifuged at 300 × g for 5 minutes prior to measurement of LDH activity in the supernatant according to the manufacturer's instructions (Roche 11644793001). The MTT solution (Promega #G3581) was diluted 1 to 5, and 50 μl was added to each well. The MTT signal (light absorbance at 570 nm) was measured 0.5 to 4 hours later using a Biotek Synergy H1 plate reader.

Human CSF and plasma samples

CSF from 6 patients with sporadic, late-onset AD, mild cognitive impairment (MCI), and age-matched neurologically normal subjects were obtained from the University of Kentucky AD Center. The latter CSF samples were drawn from living AD and MCI patients, and age-matched control subjects using standard National Alzheimer Coordinating Center and Alzheimer Disease Neuroimaging Initiative protocols. [73] Samples were from: 3 female and 3 male AD patients (age range from 74-84 years); 3 female and 3 male MCI patients (age range from 65-92 years); and 4 female and 2 male control subjects (age range from 74-83 years). CSF from 4 additional AD and 2 MCI patients as well as plasma samples were obtained from the Clinical Research Unit of the National Institute on Aging (CRU-NIA) of Harbor Hospital (Baltimore, MD). The diagnosis of AD used the criteria of probable AD as defined by the current NIA-AA criteria[74], while the diagnosis of MCI was based on the criteria set forth by the 2nd International Working Group on MCI.[75]

Calcium imaging

Neurons that had been growing on glass coverslips for 8 days were treated with EVs at indicated concentrations for 2 days. Neurons were then incubated for 20 min in the presence of Fluo 8 (0.05 ng/ml) and then washed twice with Locke's buffer. Neuronal Fluo8 fluorescence was imaged using a Zeiss LSM 510 confocal microscope. The baseline fluorescence signal was recorded for 40-100 seconds, 100 μM glutamate was then added, and the fluorescence signal was measured for at least an additional 400 seconds.

Isolation of extracellular vesicles

CSF or plasma (0.5 ml) samples were centrifuged at 2,300 × g for 30 min to remove cell debris. The supernatant was transferred to a Beckman ultracentrifugation tube (#326823) and diluted with 3 ml sterile filtered (0.22 μm filter Millex #SLG5033SS) PBS prior to centrifugation for 2.5 hours at 120,000 × g (SW55 rotor K=48). The supernatant was carefully removed and the pellet was re-suspended in lysis buffer for protein quantification or Neurobasal medium for functional assays. Rat and human neurons were grown without serum, and H4 neuroblastoma cells were washed with PBS and medium replaced with EV-depleted FBS prior to treatments and medium collection for isolation of EVs [73]. EVs were isolated from approximately 30 ml of medium (~25-30 million cells). The medium was centrifuged at 500 × g for 10 min to remove dead cells, then the supernatant was centrifuged at 2,300 × g for 10 min to remove cell debris and the supernatant was stored at −20°C. Once thawed (at room temperature), the medium was centrifuged at 120,000 × g for 2.5 hours (SW28 rotor K=246). Following this the supernatant was removed for use as an EV-depleted

control and the pellet was suspended in 3.5 ml sterile filtered PBS and centrifuged again at 120,000 g for 2.5 hours (SW55 rotor K=48) [29]. The supernatant was carefully removed and the pellet containing EVs was re-suspended in either lysis buffer for protein quantification or Neurobasal medium for functional assays.

EV labeling with PKH26/67

Membranes of EVs were labeled with the fluorescent probe PKH26 using a kit purchased from Sigma (#PKH26GL). EV pellets were suspended in 100 μl of buffer C prior to addition of 100 μl 2X PKH26 solution and incubated for 2 minutes, followed by addition of PBS containing 2% BSA (Sigma #A-3912). The labeled EVs were centrifuged twice at 120,000 × g for 1 hour (SW55i rotor K=48) with an intervening wash to ensure removal of unbound dye. The indicated amounts of EVs were added to the cells and incubated for the 4, 6 or 24 hours. As a control, PBS with the same concentration of PKH26 was centrifuged under the same conditions and added to the cells as negative control. The internalization was quantified by confocal microscopy or usinga fluorescence plate reader.

Transmission electron microscopy (TEM)

A drop of EV preparations (suspended in PBS) was added to a freshly ionized 300 mesh formvar/carbon coated grid and incubated for 5 minutes to allow adherence of the EVs to the grid. The grid was then washed through 5-7 puddles of ddH_2O; and negatively stained in 2% aqueous uranyl acetate for 30 seconds. Images were acquired using a FEI Tecnai G2 Spirit transmission electron microscope with TWIN Lens operating at 100 kV and an Olympus Soft Imaging System Megaview III digital CCD.

Quantification of EV numbers

EV suspensions were diluted 1:20 or 1:200 to permit counting in the range of $3–15 \times 10^8$/ml with an NS500 nanoparticle tracking analysis system (NanoSight, Amesbury, UK). The EVs were visualized by their scattering of a focused laser beam and the collection of the scattered light using a standard optical microscope fitted with a CCD video camera. Five exposures of 20 s each were recorded from fields chosen randomly by a computer operating with NanoSight software, which enables measurement of EV size and numbers.

Immunofluorescence, microscopy, and image analysis

Cells were grown on glass coverslips in a 24 well plate. Following the indicated treatment, cells were washed twice with PBS and were fixed in a solution of 4% paraformaldehyde in PBS for 20 minutes. Fixed cells were incubated in blocking solution (0.3% Triton X-100 and 10% normal goat serum in PBS) for 30 min, and then incubated overnight at 4°C with antibodies against cleaved-caspase 3 (D175, Cell Signaling)), MAP2 (Hm2, Sigma M9942), Aβ (6E10 SIG39320-200). The cells were then washed three times with PBS and incubated with fluorescently-tagged anti-rabbit or anti-mouse secondary antibodies (Invitrogen) in blocking solution for 1 hour at room temperature. The cells were then washed twice with PBS and, if indicated, were stained with 0.02% Thioflavin S (Sigma T-1892) for 8 minutes and then washed 3 times with 80% ethanol, twice with water and 2 times with PBS. Nuclei were stained with 4′,6-diamidino-2-phenylindole dihydrochloride (DAPI) (Sigma #32670)

in PBS for 10 minutes. All coverslips were then washed with PBS and mounted on microscope slides in an anti-fade medium (Vector Laboratories, Burlingame, CA). Images were acquired using a Zeiss LSM 510 confocal microscope with a 40X objective. Quantification of the staining intensity and area, and evaluation of co-localization were performed using Fiji software [74].

Protein extraction and immunoblots

Cells were washed twice with sterile PBS and scraped into a 15 ml tube prior to centrifugation at 700 × g for 10 min. The supernatant was then removed and the pellet was re-suspended in 100-200μl of lysis buffer (M-PER) with protease inhibitors (Complete Mini, Sigma) and incubated on ice for 30 minutes before centrifugation at 10,000 × g for 25 minutes. The supernatant was stored at −80°C. Protein extracts from EVs was prepared by re-suspension of the EV pellet in lysis buffer (M-PER) with protease inhibitors, followed by vortexing for 10 s (samples were stored at −80°C). After thawing on ice the samples were sonicated in a water bath for 5 min and centrifuged for 25 minutes at 10,000 × g. The supernatant was transferred to a new tube and used directly or stored at −80°C. Equal amounts of protein for each sample were re-suspended in sample buffer (Life NP0008) and analyzed by polyacrylamide gel electrophoresis (Life technologies NOVEX NP0302BOX or NP0321BOX) and subsequent immunoblotting. Immunocomplexes were detected by enhanced chemiluminescence (ECL) (Pierce 32106). The following antibodies were used for immunoblots: monoclonal anti-Alix (3A9, Cell Signaling 0512015)), polyclonal anti-FLOT1 (Abcam ab133497), polyclonal anti-CD9 (H-110, Santa Cruz SC9148), anti-Aβ (6E10 SIG39320-200), and anti-mouse or anti-rabbit secondary antibodies (Jackson Laboratories 715-036-151, 711-036-152).

Statistical analysis

Results are expressed as mean and S.E.M. of the indicated number of EVs preparation or independent neuronal cultures. The differences in numbers of cells that responded to glutamate treatment was determined using Chi-squared test (χ2-test). Comparisons of Aβ concentration and ratios between EVs and EV-depleted fluids was calculated by Mann-Whitney U test, unless there were more than two groups and then one-way analysis of variance (ANOVA) was used. Neurotoxicity, calcium imaging and Seahorse data were evaluated using two-way analysis of variance (ANOVA) followed by the Bonferroni post hoc test. The correlation between the EVs Aβ concentration and their toxicity was determined by linear regression. These analyses were performed using the Prism software package (Graphpad Software, San Diego, CA, USA).

Supplementary Material

Refer to Web version on PubMed Central for supplementary material.

Acknowledgement

This research was supported by the Intramural Research Program of the National Institute on Aging (NIA), and by an NIA grant supporting the University of Kentucky Alzheimer's Disease Research Center (P30-AG0-28383).

References

1. Mattson MP. Pathways towards and away from Alzheimer's disease. Nature. 2004; 430:631–639. [PubMed: 15295589]
2. Karch CM, Cruchaga C, Goate AM. Alzheimer's disease genetics: from the bench to the clinic. Neuron. 2014; 83:11–26. [PubMed: 24991952]
3. Platt TL, Reeves VL, Murphy MP. Transgenic models of Alzheimer's disease: better utilization of existing models through viral transgenesis. Biochim Biophys Acta. 2013; 1832:1437–1448. [PubMed: 23619198]
4. Bezprozvanny I, Mattson MP. Neuronal calcium mishandling and the pathogenesis of Alzheimer's disease. Trends Neurosci. 2008; 31:454–463. [PubMed: 18675468]
5. Stutzmann GE, Mattson MP. Endoplasmic reticulum Ca(2+) handling in excitable cells in health and disease. Pharmacol Rev. 2011; 63:700–727. [PubMed: 21737534]
6. Mattson MP, Gleichmann M, Cheng A. Mitochondria in neuroplasticity and neurological disorders. Neuron. 2008; 60:748–766. [PubMed: 19081372]
7. Crews L, Masliah E. Molecular mechanisms of neurodegeneration in Alzheimer's disease. Hum Mol Genet. 2010; 19:R12–20. [PubMed: 20413653]
8. Krstic D, Knuesel I. Deciphering the mechanism underlying late-onset Alzheimer disease. Nat Rev Neurol. 2013; 9:25–34. [PubMed: 23183882]
9. Aguzzi A, Rajendran L. The transcellular spread of cytosolic amyloids, prions, and prionoids. Neuron. 2009; 64:783–790. [PubMed: 20064386]
10. Watts JC, et al. Serial propagation of distinct strains of Abeta prions from Alzheimer's disease patients. Proc Natl Acad Sci U S A. 2014; 111:10323–10328. [PubMed: 24982139]
11. Stohr J, et al. Purified and synthetic Alzheimer's amyloid beta (Abeta) prions. Proc Natl Acad Sci U S A. 2012; 109:11025–11030. [PubMed: 22711819]
12. Colombo E, Borgiani B, Verderio C, Furlan R. Microvesicles: novel biomarkers for neurological disorders. Front Physiol. 2012; 3:63. [PubMed: 22479250]
13. Rajendran L, et al. Emerging roles of extracellular vesicles in the nervous system. J Neurosci. 2014; 34:15482–15489. [PubMed: 25392515]
14. Rajendran L, et al. Alzheimer's disease beta-amyloid peptides are released in association with exosomes. Proc Natl Acad Sci U S A. 2006; 103:11172–11177. [PubMed: 16837572]
15. Perez-Gonzalez R, Gauthier SA, Kumar A, Levy E. The exosome secretory pathway transports amyloid precursor protein carboxyl-terminal fragments from the cell into the brain extracellular space. J Biol Chem. 2012; 287:43108–43115. [PubMed: 23129776]
16. Saman S, et al. Exosome-associated tau is secreted in tauopathy models and is selectively phosphorylated in cerebrospinal fluid in early Alzheimer disease. J Biol Chem. 2012; 287:3842–3849. [PubMed: 22057275]
17. Emmanouilidou E, et al. Cell-produced alpha-synuclein is secreted in a calcium-dependent manner by exosomes and impacts neuronal survival. J Neurosci. 2010; 30:6838–6851. [PubMed: 20484626]
18. Grad LI, et al. Intercellular propagated misfolding of wild-type Cu/Zn superoxide dismutase occurs via exosome-dependent and -independent mechanisms. Proc Natl Acad Sci U S A. 2014; 111:3620–3625. [PubMed: 24550511]
19. Fevrier B, et al. Cells release prions in association with exosomes. Proc Natl Acad Sci U S A. 2004; 101:9683–9688. [PubMed: 15210972]
20. Rajendran L, et al. Increased Abeta production leads to intracellular accumulation of Abeta in flotillin-1-positive endosomes. Neurodegener Dis. 2007; 4:164–170. [PubMed: 17596711]
21. Colombo M, Raposo G, Thery C. Biogenesis, secretion, and intercellular interactions of exosomes and other extracellular vesicles. Annu Rev Cell Dev Biol. 2014; 30:255–289. [PubMed: 25288114]
22. Takahashi RH, et al. Intraneuronal Alzheimer abeta42 accumulates in multivesicular bodies and is associated with synaptic pathology. Am J Pathol. 2002; 161:1869–1879. [PubMed: 12414533]

23. Yuyama K, Sun H, Mitsutake S, Igarashi Y. Sphingolipid-modulated exosome secretion promotes clearance of amyloid-beta by microglia. J Biol Chem. 2012; 287:10977–10989. [PubMed: 22303002]
24. Yuyama K, et al. Decreased amyloid-beta pathologies by intracerebral loading of glycosphingolipid-enriched exosomes in Alzheimer model mice. J Biol Chem. 2014; 289:24488–24498. [PubMed: 25037226]
25. Yuyama K, et al. A potential function for neuronal exosomes: sequestering intracerebral amyloid-beta peptide. FEBS Lett. 2015; 589:84–88. [PubMed: 25436414]
26. An K, et al. Exosomes neutralize synaptic-plasticity-disrupting activity of Abeta assemblies in vivo. Mol Brain. 2013; 6:47. [PubMed: 24284042]
27. Fiandaca MS, et al. Identification of preclinical Alzheimer's disease by a profile of pathogenic proteins in neurally derived blood exosomes: A case-control study. Alzheimer's & dementia : the journal of the Alzheimer's Association. 2014
28. Wolfe DM, et al. Autophagy failure in Alzheimer's disease and the role of defective lysosomal acidification. Eur J Neurosci. 2013; 37:1949–1961. [PubMed: 23773064]
29. Witwer KW, et al. Standardization of sample collection, isolation and analysis methods in extracellular vesicle research. J Extracell Vesicles. 2013; 2
30. Lotvall J, et al. Minimal experimental requirements for definition of extracellular vesicles and their functions: a position statement from the International Society for Extracellular Vesicles. J Extracell Vesicles. 2014; 3:26913. [PubMed: 25536934]
31. Spies PE, et al. The cerebrospinal fluid amyloid beta42/40 ratio in the differentiation of Alzheimer's disease from non-Alzheimer's dementia. Curr Alzheimer Res. 2010; 7:470–476. [PubMed: 20043812]
32. Sauvee M, et al. Additional use of Abeta(4)(2)/Abeta(4)(0) ratio with cerebrospinal fluid biomarkers P-tau and Abeta(4)(2) increases the level of evidence of Alzheimer's disease pathophysiological process in routine practice. J Alzheimers Dis. 2014; 41:377–386. [PubMed: 24614902]
33. Mahairaki V, et al. Induced pluripotent stem cells from familial Alzheimer's disease patients differentiate into mature neurons with amyloidogenic properties. Stem Cells Dev. 2014; 23:2996–3010. [PubMed: 25027006]
34. Bulloj A, Leal MC, Xu H, Castano EM, Morelli L. Insulin-degrading enzyme sorting in exosomes: a secretory pathway for a key brain amyloid-beta degrading protease. J Alzheimers Dis. 2010; 19:79–95. [PubMed: 20061628]
35. Ghidoni R, et al. Cystatin C is released in association with exosomes: a new tool of neuronal communication which is unbalanced in Alzheimer's disease. Neurobiol Aging. 2011; 32:1435–1442. [PubMed: 19773092]
36. Yuyama K, Yamamoto N, Yanagisawa K. Accelerated release of exosome-associated GM1 ganglioside (GM1) by endocytic pathway abnormality: another putative pathway for GM1-induced amyloid fibril formation. J Neurochem. 2008; 105:217–224. [PubMed: 18021298]
37. Thinakaran G, Koo EH. Amyloid precursor protein trafficking, processing, and function. J Biol Chem. 2008; 283:29615–29619. [PubMed: 18650430]
38. Vingtdeux V, et al. Intracellular pH regulates amyloid precursor protein intracellular domain accumulation. Neurobiol Dis. 2007; 25:686–696. [PubMed: 17207630]
39. Haass C, Capell A, Citron M, Teplow DB, Selkoe DJ. The vacuolar H(+)-ATPase inhibitor bafilomycin A1 differentially affects proteolytic processing of mutant and wild-type beta-amyloid precursor protein. J Biol Chem. 1995; 270:6186–6192. [PubMed: 7890753]
40. Mattson MP, et al. beta-Amyloid peptides destabilize calcium homeostasis and render human cortical neurons vulnerable to excitotoxicity. J Neurosci. 1992; 12:376–389. [PubMed: 1346802]
41. Xin H, et al. Systemic administration of exosomes released from mesenchymal stromal cells promote functional recovery and neurovascular plasticity after stroke in rats. J Cereb Blood Flow Metab. 2013; 33:1711–1715. [PubMed: 23963371]
42. Borchelt DR, et al. Accelerated amyloid deposition in the brains of transgenic mice coexpressing mutant presenilin 1 and amyloid precursor proteins. Neuron. 1997; 19:939–945. [PubMed: 9354339]

43. Oddo S, et al. Triple-transgenic model of Alzheimer's disease with plaques and tangles: intracellular Abeta and synaptic dysfunction. Neuron. 2003; 39:409–421. [PubMed: 12895417]
44. Dumurgier J, et al. Cerebrospinal fluid amyloid-beta 42/40 ratio in clinical setting of memory centers: a multicentric study. Alzheimers Res Ther. 2015; 7:30. [PubMed: 26034513]
45. Kuperstein I, et al. Neurotoxicity of Alzheimer's disease Abeta peptides is induced by small changes in the Abeta42 to Abeta40 ratio. EMBO J. 2010; 29:3408–3420. [PubMed: 20818335]
46. Pauwels K, et al. Structural basis for increased toxicity of pathological abeta42:abeta40 ratios in Alzheimer disease. J Biol Chem. 2012; 287:5650–5660. [PubMed: 22157754]
47. Fiandaca MS, et al. Identification of preclinical Alzheimer's disease by a profile of pathogenic proteins in neurally derived blood exosomes: A case-control study. Alzheimer's & dementia : the journal of the Alzheimer's Association. 2015; 11:600–607. e601.
48. Kokubo H, et al. Oligomeric proteins ultrastructurally localize to cell processes, especially to axon terminals with higher density, but not to lipid rafts in Tg2576 mouse brain. Brain Res. 2005; 1045:224–228. [PubMed: 15910781]
49. Williamson R, Usardi A, Hanger DP, Anderton BH. Membrane-bound beta-amyloid oligomers are recruited into lipid rafts by a fyn-dependent mechanism. FASEB J. 2008; 22:1552–1559. [PubMed: 18096814]
50. Rushworth JV, Hooper NM. Lipid Rafts: Linking Alzheimer's Amyloid-beta Production, Aggregation, and Toxicity at Neuronal Membranes. Int J Alzheimers Dis. 2010; 2011:603052. [PubMed: 21234417]
51. Evangelisti E, et al. Lipid rafts mediate amyloid-induced calcium dyshomeostasis and oxidative stress in Alzheimer's disease. Curr Alzheimer Res. 2013; 10:143–153. [PubMed: 22950913]
52. Laulagnier K, et al. Mast cell- and dendritic cell-derived exosomes display a specific lipid composition and an unusual membrane organization. Biochem J. 2004; 380:161–171. [PubMed: 14965343]
53. Butterfield DA, Hensley K, Harris M, Mattson M, Carney J. beta-Amyloid peptide free radical fragments initiate synaptosomal lipoperoxidation in a sequence-specific fashion: implications to Alzheimer's disease. Biochem Biophys Res Commun. 1994; 200:710–715. [PubMed: 8179604]
54. Bruce-Keller AJ, et al. Bcl-2 protects isolated plasma and mitochondrial membranes against lipid peroxidation induced by hydrogen peroxide and amyloid beta-peptide. J Neurochem. 1998; 70:31–39. [PubMed: 9422344]
55. Keller JN, et al. Impairment of glucose and glutamate transport and induction of mitochondrial oxidative stress and dysfunction in synaptosomes by amyloid beta-peptide: role of the lipid peroxidation product 4-hydroxynonenal. J Neurochem. 1997; 69:273–284. [PubMed: 9202320]
56. Mark RJ, Pang Z, Geddes JW, Uchida K, Mattson MP. Amyloid beta-peptide impairs glucose transport in hippocampal and cortical neurons: involvement of membrane lipid peroxidation. J Neurosci. 1997; 17:1046–1054. [PubMed: 8994059]
57. Mark RJ, Lovell MA, Markesbery WR, Uchida K, Mattson MP. A role for 4-hydroxynonenal, an aldehydic product of lipid peroxidation, in disruption of ion homeostasis and neuronal death induced by amyloid beta-peptide. J Neurochem. 1997; 68:255–264. [PubMed: 8978733]
58. Tamboli IY, et al. Statins promote the degradation of extracellular amyloid {beta}-peptide by microglia via stimulation of exosome-associated insulin-degrading enzyme (IDE) secretion. J Biol Chem. 2010; 285:37405–37414. [PubMed: 20876579]
59. Pasternak SH, Callahan JW, Mahuran DJ. The role of the endosomal/lysosomal system in amyloid-beta production and the pathophysiology of Alzheimer's disease: reexamining the spatial paradox from a lysosomal perspective. J Alzheimers Dis. 2004; 6:53–65. [PubMed: 15004328]
60. Shen B, Wu N, Yang JM, Gould SJ. Protein targeting to exosomes/microvesicles by plasma membrane anchors. J Biol Chem. 2011; 286:14383–14395. [PubMed: 21300796]
61. Abache T, et al. The transferrin receptor and the tetraspanin web molecules CD9, CD81, and CD9P-1 are differentially sorted into exosomes after TPA treatment of K562 cells. J Cell Biochem. 2007; 102:650–664. [PubMed: 17407154]
62. Andreu Z, Yanez-Mo M. Tetraspanins in extracellular vesicle formation and function. Front Immunol. 2014; 5:442. [PubMed: 25278937]

63. Baietti MF, et al. Syndecan-syntenin-ALIX regulates the biogenesis of exosomes. Nat Cell Biol. 2012; 14:677–685. [PubMed: 22660413]

64. Cataldo AM, Hamilton DJ, Nixon RA. Lysosomal abnormalities in degenerating neurons link neuronal compromise to senile plaque development in Alzheimer disease. Brain Res. 1994; 640:68–80. [PubMed: 8004466]

65. Cataldo AM, Nixon RA. Enzymatically active lysosomal proteases are associated with amyloid deposits in Alzheimer brain. Proc Natl Acad Sci U S A. 1990; 87:3861–3865. [PubMed: 1692625]

66. Lee JH, et al. Lysosomal proteolysis and autophagy require presenilin 1 and are disrupted by Alzheimer-related PS1 mutations. Cell. 2010; 141:1146–1158. [PubMed: 20541250]

67. Nixon RA, et al. Extensive involvement of autophagy in Alzheimer disease: an immuno-electron microscopy study. J Neuropathol Exp Neurol. 2005; 64:113–122. [PubMed: 15751225]

68. Pickford F, et al. The autophagy-related protein beclin 1 shows reduced expression in early Alzheimer disease and regulates amyloid beta accumulation in mice. J Clin Invest. 2008; 118:2190–2199. [PubMed: 18497889]

69. Nilsson P, et al. Abeta secretion and plaque formation depend on autophagy. Cell Rep. 2013; 5:61–69. [PubMed: 24095740]

70. Goetzl EJ, et al. Altered lysosomal proteins in neural-derived plasma exosomes in preclinical Alzheimer disease. Neurology. 2015; 85:40–47. [PubMed: 26062630]

71. Swerdlow RH. Alzheimer's disease pathologic cascades: who comes first, what drives what. Neurotox Res. 2012; 22:182–194. [PubMed: 21913048]

72. Mattson MP, Barger SW, Begley JG, Mark RJ. Calcium, free radicals, and excitotoxic neuronal death in primary cell culture. Methods Cell Biol. 1995; 46:187–216. [PubMed: 7541884]

73. Eitan E, Zhang S, Witwer KW, Mattson MP. Extracellular vesicle-depleted fetal bovine and human sera have reduced capacity to support cell growth. J Extracell Vesicles. 2015; 4:26373. [PubMed: 25819213]

74. Schindelin J, et al. Fiji: an open-source platform for biological-image analysis. Nat Methods. 2012; 9:676–682. [PubMed: 22743772]

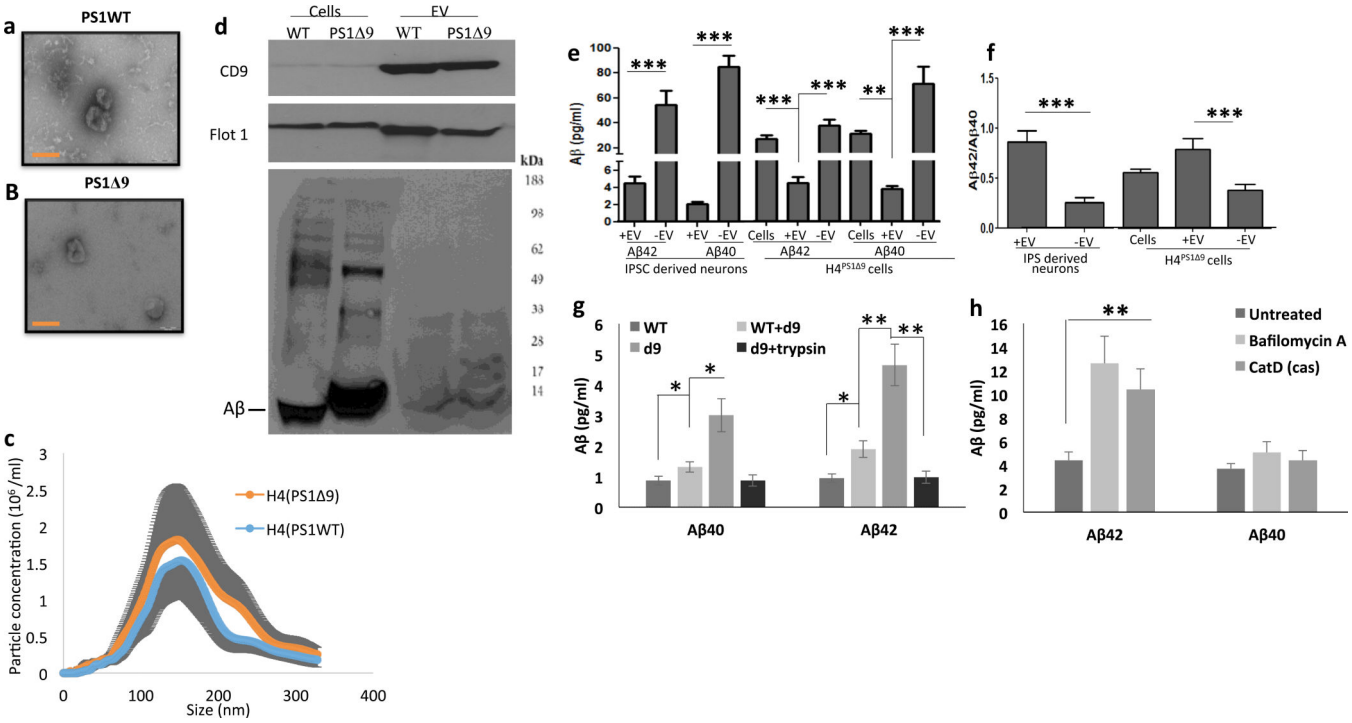

Figure 1.

Human neural cells expressing familial AD presenilin 1 mutations release extracellular vesicles (EVs) with elevated levels of Aβ42 on their outer surface. **A and B.** Transmission electron microscope images of EVs released from H4 cells expressing either the δ9 PS1 mutation (A) or wild type (WT) PS1 (B). Scale bar = 100 nm. **C.** Size distribution of EVs released from H4 cells expressing mutant or wild type PS1 measured by Nanocyte particle tracking. **D**. Immunoblot demonstrating enrichment of EV markers CD9 and Flotillin-1 in EVs released from H4 cells, and relatively low amounts of Aβ in EVs relative to H4 cell lysate. **E and F.** Levels of Aβ42 and Aβ40 (E) and the Aβ42/Aβ40 ratio (F) in cells, EVs and EV-depleted medium from neurons differentiated from iPSC that were generated from fibroblasts from a patient with familial AD (PS1 mutation; n=5 cultures), and from H4 human neuroglioma cells expressing mutant PS1 (8 separate cultures). **G.** Levels of Aβ40 and Aβ42 in EVs isolated from the medium of cultured H4Ps1Δ9 cells, H4Ps1WT cells, H4Ps1WT EVs incubated in H4Psn1Δ9 EV-depleted medium, or H4Psn1Δ9 EVs incubated with trypsin (n = 3). **H.** Levels of Aβ40 and Aβ42 in EVs isolated from the medium of cultured H4Psn1Δ9 cells that had been treated for 24 hours with vehicle (control; n = 5) or bafilomycin A (n = 5), or in which cathepsin D was knocked down using CRISPR Cas9 technology (n = 3). *p < 0.05, **p < 0.01, ***p < 0.001.

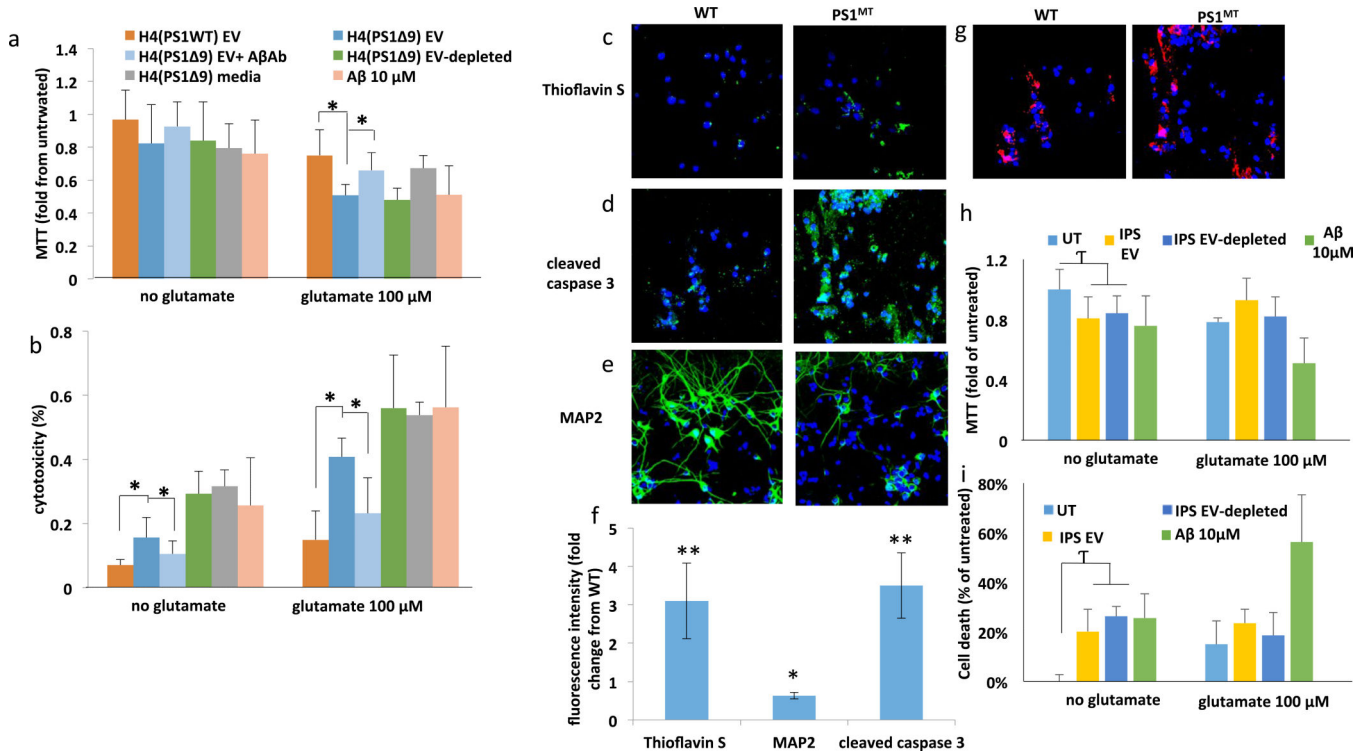

Figure 2.

EVs isolated from the medium of cultured human neural cells expressing mutant PS1 are neurotoxic. **A and B.** Rat primary cortical neurons were exposed to the indicated treatments for 24 hours and cell viability was evaluated by MTT (A) and LDH (B) assays (n = 3-6 separate cultures). **C.** Thioflavin S (green), and DAPI (blue) staining demonstrates that treating cortical neuron cultures with Psn1Δ9-derived EVs results in the accumulation of Thioflavin S reactive aggregates. **D.** Cleaved caspase 3 staining (green) and DAPI (blue) staining showing increased cell death following incubation of cortical neuron cultures with Psn1Δ9-derived but not WT EVs. **E.** Reduced MAP2 staining (green; a neuronal protein) is observed in rat neuronal cultures incubated with Psn1Δ9-derived EVs. DAPI (blue). **F.** Quantification of fluorescence intensities of primary neuronal cultures that had been exposed for 48 hours to EVs derived from H4 cells expressing mutant PS1 and then stained with Thioflavin S, cleaved caspase 3 and MAP2. Values are expressed as fold difference from the value for neurons exposed to EVs from control H4 cells (n = 6 cultures). **G.** Images showing PKH-labeled EVs (red) and DAPI (blue) staining in cortical neurons that had been incubated for 6 hours in the presence of EVs released from H4 cells expressing WT PS1 Psn1Δ9 PS1. **H and I.** Levels of MTT reduction and LDH release (cytotoxicity) in cortical neurons that that had been incubated for 48 hours in the presence of EVs from neurons derived from iPSC generated from fibroblasts from a patient with familial AD (IPS), EV-depleted iPSC culture medium, or Aβ1-42 (10 μM). UT, untreated control cultures. Cultures were co-treated with glutamate (100 nM) or vehicle as indicated. Values are the mean and SEM (n = 6 cultures). *p < 0.05, **p < 0.01.

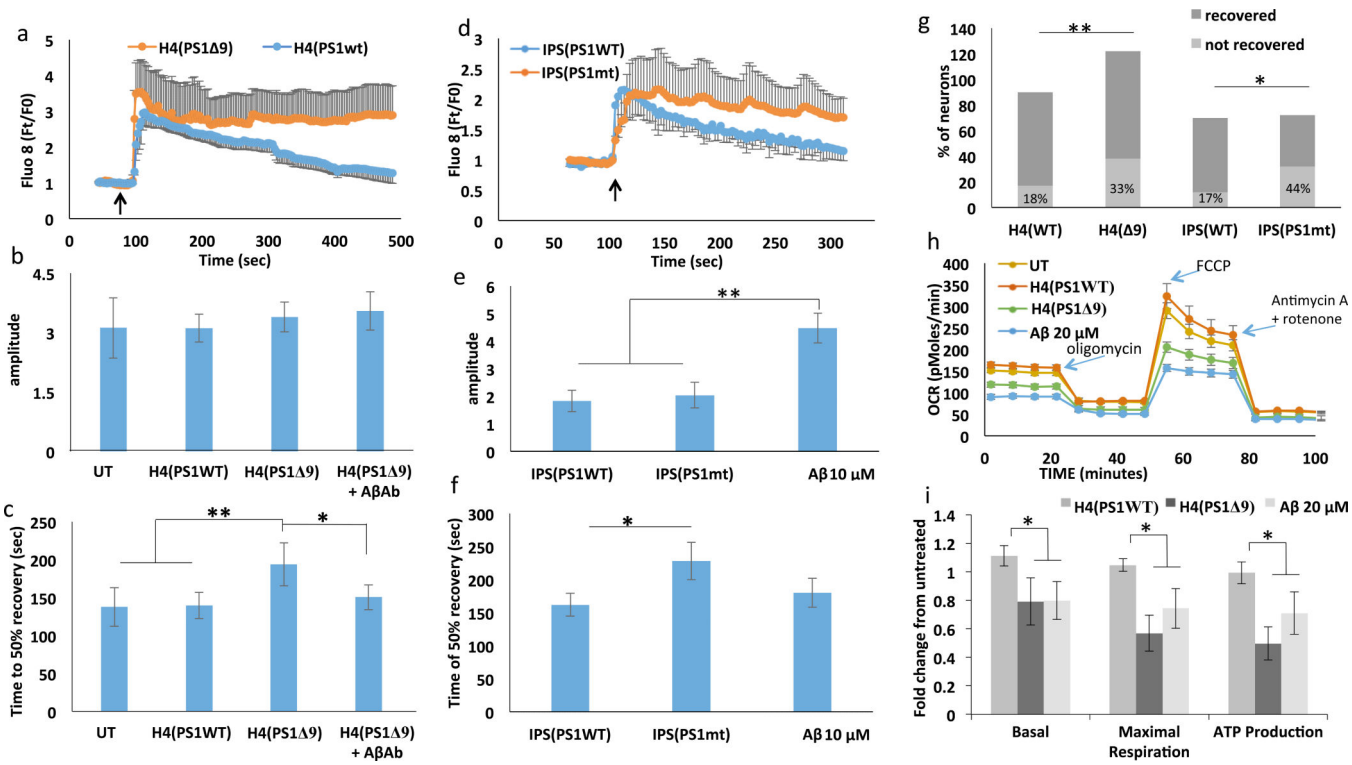

Figure 3.

EVs generated by human neural cells expressing mutant PS1 impair cellular Ca^{2+} handling and mitochondrial function in cerebral cortical neurons. **A.** Preincubation of rat cortical neurons with H4Psn1Δ9-derived EVs for 24 hours resulted in a greater sustained Ca^{2+} response to glutamate (10 μM) stimulation (arrow indicates the time of glutamate application) compared to neurons preincubated with EVs from H4Psn1WT cells. Values are the mean and SEM of measurements made in 20 neurons per culture in 7 different cultures. **B and C.** Quantification of peak amplitude (B) and time to reach 50% recovery (B) following glutamate stimulation in cortical neurons that had been pretreated for 24 hours with EVs (H4D9 cells with either WT or Δ9 PS1; H4(PS1Δ9)+AβAb was a condition in which the EVs were incubated with an Aβ antibody (6E10). Values are the mean and SEM of measurements made in neurons from 7 different cultures. **D.** AD patient iPSC-derived neuronal EVs induce Ca^{2+} dysregulation following stimulation with glutamate (10 μM; arrow indicates the time of glutamate application). Values are the mean and SEM of measurements made in 3 different cultures (20 neurons per culture). **E and F.** Peak amplitude (E), and time to reach 50% recovery (F) following glutamate stimulation in rat cortical neurons pretreated for 24 hours with EVs from AD patient or WT iPSC-derived neurons (Aβ condition is rat cortical neurons incubated with 10 μM synthetic Aβ1-42). **G.** Analysis of the percentage of cortical neurons unresponsive to glutamate following incubation with mutant or WT EVs derived from H4 cells and IPSC-derived neurons (n =7 for H4 EVs treated neurons and n=3 for IPC EVs treated neurons). **H.** Representative Seahorse oxygen consumption assay showing mitochondrial impairment 24 hours following treatment with H4Psn1Δ9-derived EVs or 20 μM Aβ1-42. **I.** Basal oxygen consumption rate, maximal consumption rate and ATP production in cortical neurons that had been treated for

24 hours with H4Psn1Δ9-derived EVs or 20 μM Aβ1-42. Values are the mean and SEM from measurements made in 5 independent cultures. *p<0.05, **p<0.01.

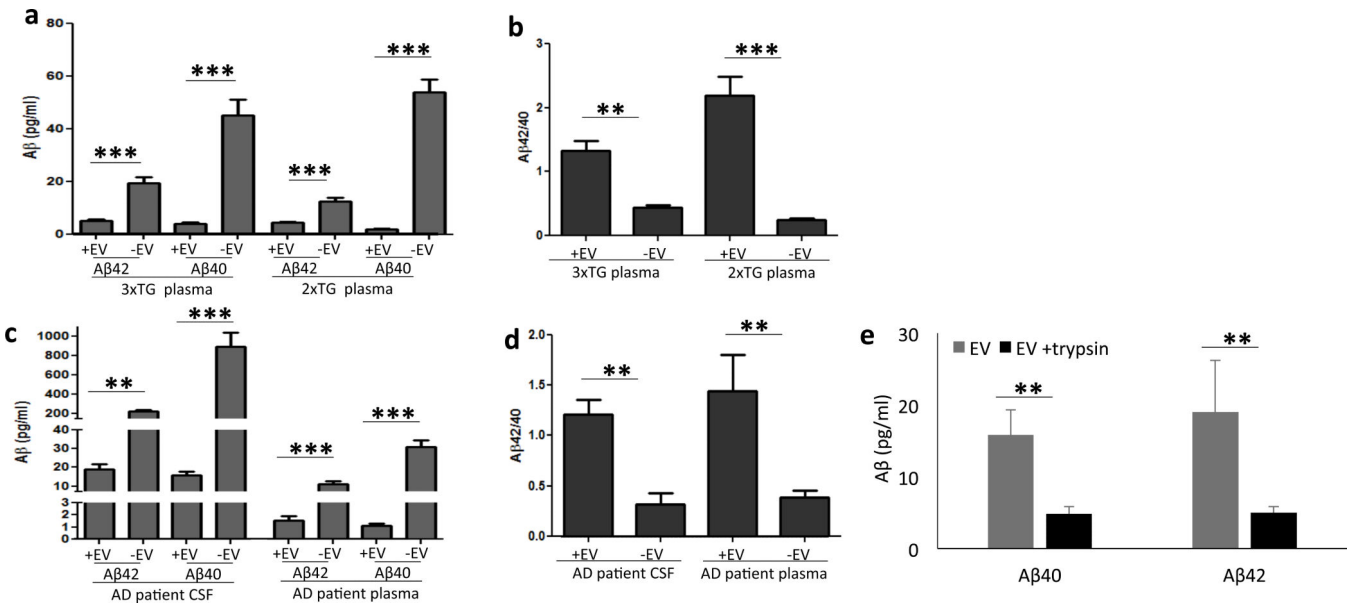

Figure 4.

EVs isolated from CSF and plasma of AD patients, and from plasma in two AD mouse models, exhibit a high Aβ42/40 ratio. Concentrations of Aβ40 and Aβ42 were measured in samples of EVs (+EV) and corresponding fluids from which they were isolated (−EV). **A and B.** Results of analyses of blood plasma samples from 3xTgAD and 2xTgAD mice (n =5 3xTgAD and n=6 2xTgAD mice). **C and D.** Results of analyses of CSF and blood plasma samples from AD patients. (n = 6 patients). **E.** Quantification of Aβ40 and Aβ42 levels in EVs isolated from the CSF of AD patients. The EVs were incubated with or without with trypsin to prior to the analysis (EV preparations from 3 different AD patients). **p < 0.01, ***p < 0.001.

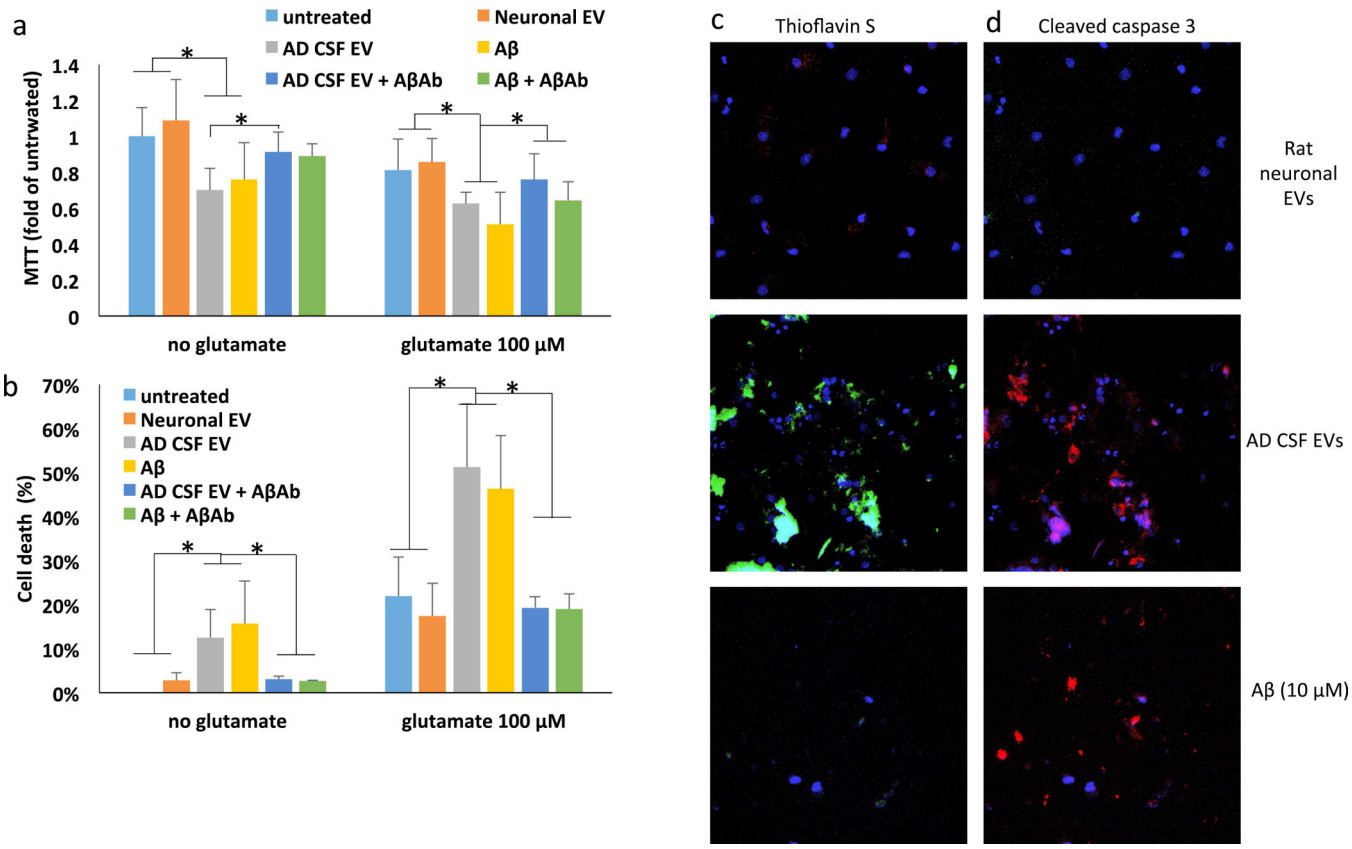

Figure 5.

AD patient CSF-derived EVs are neurotoxic. **A and B.** Results of MTT and LDH assays demonstrating that 48 h incubation of rat neurons with AD CSF EVs (at a concentration of 100 EVs per neuron) diminished neuronal survival by an amount similar to that of neurons exposed to Aβ1-42 (10 μM). AD CSF EVs also increased neuronal vulnerability to glutamate during a 24 h incubation (n = 6 cultures). Where indicated, cultures were co-treated with Aβ antibody 6E10 (1 μg antibody per 10^7 EVs). **C and D.** Cultured cortical neurons were incubated for 24 hours in the presence of fluorescently tagged EVs that had been isolated from the culture medium of rat cortical neurons or from AD CSF (100 EVs per neuron), or with 10 μM Aβ1-42. Cortical neurons were then stained with Thioflavin S or anti-cleaved caspase 3. Representative images are shown. Similar results were obtained in 6 separate experiments. *$p<0.05$.

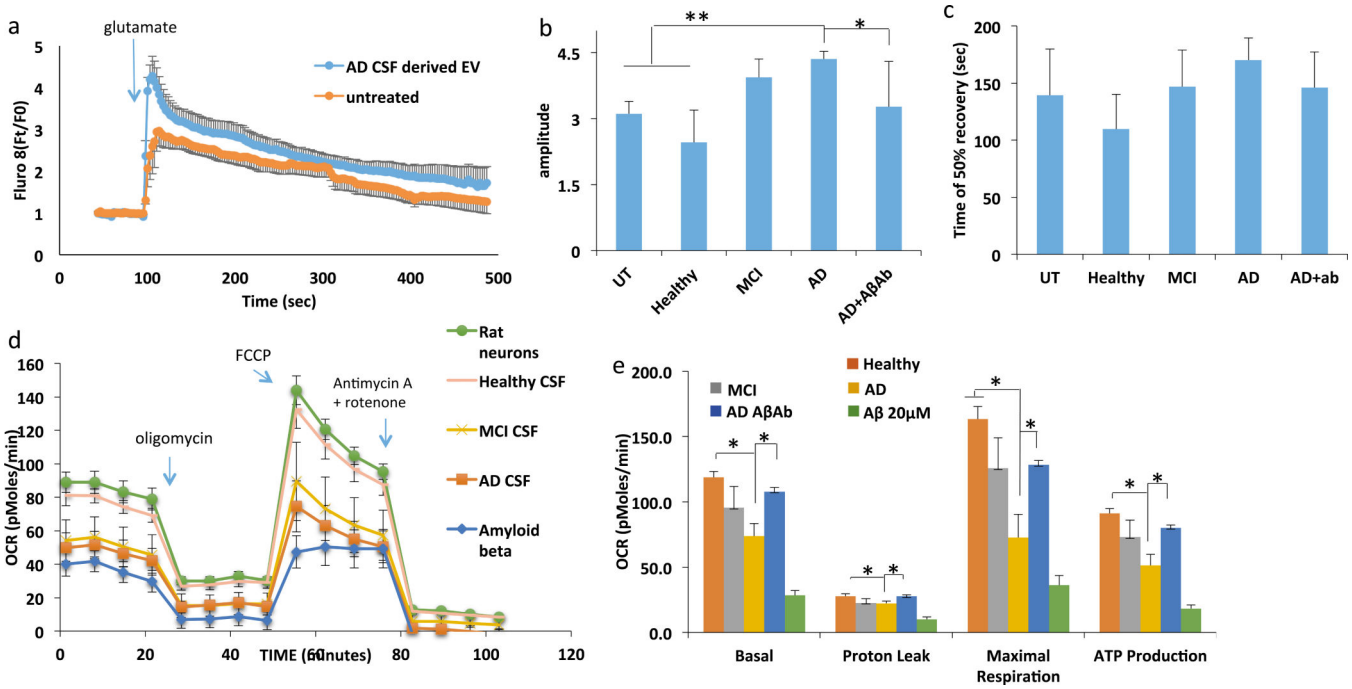

Figure 6.

AD patient CSF-derived EVs impair neuronal Ca^{2+} regulation and mitochondrial function. **A.** Graph showing relative intracellular Ca^{2+} levels (Fluo 8 fluorescence intensity before and during exposure to glutamate (100 μM). **B and C.** Graphs showing amplitudes of peak Ca^{2+} responses to glutamate (B) and the time required for the Fluo 8 fluorescence intensity to recover to 50% of the peak level (C). **D and E.** Results of Seahorse analysis of mitochondrial respiration in cultured neurons that had been pretreated for 24 h with EVs isolated from the medium bathing healthy primary rat cortical neurons (100 particles per neuron), 10 μM Aβ or EVs isolated from the CSF of AD patients (100 particles per neuron). Panel D shows results of a representative experiment and panel E shows data from 6 experiments. *p<0.05; **p<0.01.